Published in final edited form as:
Biomaterials. 2013 October ; 34(31): 7766–7775. doi:10.1016/j.biomaterials.2013.06.039.

Mechanisms of monoclonal antibody stabilization and release from silk biomaterials

Nicholas A. Guziewicz[a,1], **Andrew J. Massetti**[a], **Bernardo J. Perez-Ramirez**[a], and **David L. Kaplan**[b,*]

[a]BioFormulations Development, Genzyme, A Sanofi Company, 1 Mountain Road, P.O. Box 9322, Framingham, MA 01701-9322, USA

[b]Department of Biomedical Engineering, School of Engineering, Tufts University, 4 Colby St, Medford, MA 02155, USA

Abstract

The availability of stabilization and sustained delivery systems for antibody therapeutics remains a major clinical challenge, despite the growing development of antibodies for a wide range of therapeutic applications due to their specificity and efficacy. A mechanistic understanding of protein-matrix interactions is critical for the development of such systems and is currently lacking as a mode to guide the field. We report mechanistic insight to address this need by using well-defined matrices based on silk gels, in combination with a monoclonal antibody. Variables including antibody loading, matrix density, charge interactions, hydrophobicity and water access were assessed to clarify mechanisms involved in the release of antibody from the biomaterial matrix. The results indicate that antibody release is primarily governed by hydrophobic interactions and hydration resistance, which are controlled by silk matrix chemistry, peptide domain distribution and protein density. Secondary ionic repulsions are also critical in antibody stabilization and release. Matrix modification by free methionine incorporation was found to be an effective strategy for mitigating encapsulation induced antibody oxidation. Additionally, these studies highlight a characterization approach to improve the understanding and development of other protein sustained delivery systems, with broad applicability to the rapidly developing monoclonal antibody field.

Keywords

Protein; Antibody; Stability; Sustained delivery; Silk; Hydrogel

1. Introduction

Sustained local delivery of drugs offers many advantages over systemic delivery. The most obvious advantage is the potential for improved efficacy, by maintaining drug levels within the therapeutic window for longer periods of time [1]. Also, delivering drugs directly to the disease site eliminates the dependence on physiological targeting mechanisms and provides higher levels of therapeutic available at the targeted site [2,3]. Monoclonal antibodies are excellent therapeutic targets due to their specificity, modular structure, ability to leverage the patient's own immune system, and ability to deliver a toxic payload [4-6]. Antibody

*Corresponding author. Tel.: +1 617 627 3251; fax: +1 617 627 3231. david.kaplan@tufts.edu (D.L. Kaplan). .
[1]Current address: Drug Product Process Technology, Amgen Inc., One Amgen Center Drive, Thousand Oaks, CA 91320, USA.

based therapies are being developed for a wide range of indications in oncology, inflammation, immune mediated disorders, and wound healing [7]. Long-term repetitive dosing is common for antibody therapies, therefore drug efficacy and patient compliance would benefit significantly from the availability of sustained local delivery options [7]. While numerous systems and devices are available for sustained local delivery of small molecule therapeutics, none currently exist for monoclonal antibodies despite their broad therapeutic appeal [8]. The limited availability of sustained local delivery systems for antibody therapeutics can be attributed to two factors: material/processing incompatibility with proteins and a flawed development approach.

First, the challenges in manufacturing inherently unstable protein therapeutics are exaggerated if a combination therapy is being developed [8]. The materials and processing strategies commonly used for engineering delivery systems for proteins have drawbacks, limiting their utility. Organic solvents, chemical cross-linking agents, pH extremes, mechanical stress, and acidic degradation products are frequently required or are present [9-11]. While often acceptable for small molecule therapeutics, these processing strategies are typically incompatible with relatively fragile protein therapeutics [12,13].

Second, and perhaps more importantly, there are limitations to the approach employed for development of combination products, namely the independent development and optimization paths for protein therapeutic and delivery matrices. Each product itself is complex and unique, requiring years of characterization, optimization, and engineering. It is unlikely that an after-the-fact merging of a protein therapeutic with an “off-the-shelf” delivery matrix would be successful. Considering the nuances of each product, incompatibilities and instabilities emerge. The ideal approach would involve co-development of a protein therapeutic with its intended delivery matrix. In this approach, as incompatibilities or instabilities are identified, opportunities exist for matrix or protein optimization to improve the probability of success. Also, the nature of antibody-matrix interactions must be thoroughly understood in order to optimize release profiles. The delivery matrix should be optimized for a specific protein therapeutic and vice versa.

While there are many types of biomaterials potentially useful for the above needs, silk fibroin has the potential to address some of these limitations. Silk fibroin is a naturally occurring protein polymer which can be processed into a wide range of useful biomaterial formats including sponges, films, micro/nanoparticles, coatings and hydrogels with a high degree of control of structure and morphology [14]. The use of silk fibroin as a versatile biomaterial, specifically its biocompatibility, all aqueous and ambient manufacturing process, controllable degradation rates, impressive mechanical properties and favorable immunological properties are well documented [14-17]. Specifically, silk-based materials have been successfully used for sustained small molecule and protein delivery in addition to enzyme, antibiotic, and vaccine stabilization [18-24].

The studies presented here demonstrate the criticality of thorough antibody-matrix interaction characterization. Recently, silk fibroin lyogels, a novel matrix for sustained local delivery of monoclonal antibodies, was described [25]. In order to engineer silk lyogels to optimize antibody release profiles, recovery and stability, insight into the mechanisms governing silk-solvent and silkantibody interactions was required. Such insights offer to further refine this stabilization and delivery protocol for antibodies in silk matrices. The current work describes a series of mechanistic studies on antibody loaded silk lyogels. The relationship between silk density, hydration behavior, and antibody recovery was confirmed and characterized. Release studies were used to characterize the nature of silk-antibody interactions, a surfactant was used to evaluate the role of hydrophobic interactions and hydration behavior, and salt and pH studies were used to probe ionic interactions. The

impact of encapsulation on antibody stability was also evaluated and damage mitigation strategies were developed. Finally, a unified mechanism describing the factors that impact antibody release from silk lyogels is proposed. This approach serves as a model for characterization of other antibody-matrix systems, with broad implications in facilitating successful development of such delivery systems.

2. Materials and methods

2.1. Materials

Bombyx mori silkworm cocoons were purchased from Tajima Shoji Co., LTD (Sumiyashicho, Naka-Ku, Yokohama, Japan) and used to produce silk fibroin solutions [14]. All studies were conducted using purified murine Immunoglobulin G type 1 (IgG1) monoclonal antibody provided by Genzyme Corporation (Framingham, MA). All chemicals used in the production of silk and the preparation of solutions were reagent grade and purchased from either SigmaeAldrich (St. Louis, MO) or Mallinckrodt Baker, Inc. (Phillipsburg, NJ). Lyophilization of the antibody was performed in clear type I borosilicate glass serum vials obtained from Wheaton Industries, Inc. (Millville, NJ). All aqueous solutions were prepared using ultrapure water (UPW) with <5 ppb total organic carbon (TOC) and an 18.2 MU resistivity produced by a Millipore Milli-Q Advantage A10 purification system (Billerica, MA).

2.2. Lyophilized antibody powders

Antibody solutions at 5 mg mL^{-1} formulated in 0.02 M histidine buffer, 0.5% (w/v) sucrose, pH 6.0 were lyophilized in a LyoStarII tray freeze dryer (FTS Systems, Stone Ridge, NY) according to previously established procedures [25]. Lyophilized antibody samples were stored at 5° ± 3 °C prior to use.

2.3. Preparation of silk hydrogels and lyogels

Concentrated silk fibroin solutions were produced using the 60 min boil aqueous process described by Rockwood et al. [14]. Silk hydrogels and lyogels were prepared by sonication and subsequent lyophilization [25]. For antibody-containing hydrogels and lyogels, lyophilized antibody powder was added to the sonicated solutions to a target concentration of 5 mg mL^{-1}. Methionine loaded lyogels were produced by spiking 10× methionine solutions into sonicated silk. Lyogels were pressed into discs using a 12-ton EZ press and 6 mm and 13 mm die sets (Crystal Laboratories International, Garfield, NJ). The lyogels were pressed with the 6 mm die at 1000 psi for 10 s. Some samples were pressed a second time with the 13 mm die at 2500 psi for 10 s.

2.4. Swelling properties

The swelling properties of each lyogel were tracked at each time point. Prior to transferring the lyogel to fresh release medium, excess buffer was removed from the lyogel by contact with the inside surface to the polystyrene vial and the weight of the rehydrated lyogel was determined (W_r). The swelling ratio was calculated using Equation (1),

$$\text{Swelling ratio} = \frac{W_r - W_d}{W_d} \quad (1)$$

where $W_d$is the mass of the dried lyogel. The reported swelling ratio is the first mass reading after a plateau in fluid uptake was observed, typically after 1–2 days.

2.5. Silk matrix characterization

Secondary structure of the silk matrix was analyzed by Fourier transform infrared spectroscopy (FTIR) on an MB series spectrometer (ABB Bomem, Quebec, Canada) equipped with a MIRacle attenuated total reflection (ATR) diamond crystal (Pike Technologies, Madison, WI). Data acquisition and analysis were performed using PROTA (BioTools, Inc., Jupiter, FL) together with RazorTools 6.0 (Spectrum Square Associates, Inc., Ithaca, NY). Fourier self-deconvolution (FSD) of the amide I region (1590–1710 cm^{-1}) was performed to quantify secondary structure composition. Experiments and data analysis were executed using previously established procedures [25-28]. Thermal properties of silk lyogels were investigated using temperature modulated differential scanning calorimetry (TMDSC) on a Q2000 DSC equipped with the RCS90 refrigeration system (TA Instruments, New Castle, DE). The instrument was operated with a nitrogen purge at 50 mL min^{-1}. Calibration for temperature was performed using indium and for heat capacity using sapphire. Silk lyogel samples, 5–10 mg, were loaded into Tzero aluminum pans (TA Instruments, New Castle, DE) and sealed. The samples were heated at 2 °C min^{-1} from −40 °C to 350 °C with a modulation period of 60 s and temperature amplitude of 0.318 °C.

2.6. Antibody characterization

Physical and chemical stability characterization methods for antibodies such as size exclusion chromatography (SEC), circular dichroism (CD), sodium dodecyl sulfate polyacrylamide gel electrophoresis (SDS-PAGE), isoelectric focusing polyacrylamide gel electrophoresis (IEF-PAGE), and peptide mapping are well established procedures and will not be described here in depth [13,29,30]. Antibody function was evaluated in a previously described potency assay based on the TGFβ-induced release of Interleukin-11 (IL-11) by the human lung epithelial cell line A549 [31].

2.7. Statistical analysis

Each data point is the average of five individual lyogels in a specified release medium and is reported ± standard deviation (SD), unless noted otherwise.

3. Results

3.1. Antibody release from variable density silk lyogels

The impact of silk density on IgG1 monoclonal antibody release was evaluated. Initially, 1.0 mg of lyophilized antibody was loaded at a target concentration of 5 mg mL^{-1} (0.5% (w/w)) into sonicated silk solutions ranging in concentration from 3.1% (w/w) to 6.7% (w/w). In this combination, the ratio of silk to antibody increased from 6.2 to 13.4 with increasing silk density. To simulate physiological conditions, PBS at pH 7.4 was used as a release medium and was exchanged at pre-determined intervals. Antibody released was measured by protein G-ID affinity chromatography. For all release studies, data presented in the figures was truncated for simplified visualization when cumulative release approached approximately 85% of the final cumulative release observed, which is reported in the tables.

Both release rate and cumulative release amount decreased incrementally with increasing silk concentration (Fig.1A). In the 3.1% (w/w) silk lyogel samples, release was nearly complete at day eight with 79.6% of the loaded antibody recovered. In contrast, at day eight only 17.9% of the loaded antibody was released from 6.7% (w/w) silk lyogels. Antibody release from 6.7% (w/w) lyogels continued through 160 days reaching a final cumulative release of 36% (Table 1). Lyogel hydration, as measured by the swelling ratio, decreased incrementally from 16.0 to 6.7 with increasing silk concentration (Table 1). The reported swelling ratio is the first mass reading after a plateau in fluid uptake was observed, typically after 1–2 days.

Silk density was further altered by compacting 3.2% (w/w) antibody loaded silk lyogels using a hydraulic press at either 1500 or 2500 psi. This procedure increased silk density from 44.9 g $(cm^3)^{-1}$ to 1045.3 g $(cm^3)^{-1}$ and 1320.5 g $(cm^3)^{-1}$ for the low and high pressure condition, respectively (Table 1). In this composition the silk to antibody ratio remained constant at 6.4 while the silk density increased. Antibody release (Fig. 1B) and swelling ratio (Table 1) both decreased significantly in the pressed lyogel samples. Antibody release was suppressed to only 3% in the high pressure sample compared to 69.8% in the control (Table 1). The swelling ratio decreased to 0.5 for the 2500 psi sample compared to 14.5 in the control. Intermediate values for swelling ratio and antibody recovery were observed in the 1500 psi sample. Silk density versus swelling data from 19 lyogel preparations were compared (Fig. 1C) to further characterize this relationship. Increasing silk density significantly decreased the swelling ratio of silk lyogels. Silk densities below 200 g $(cm^3)^{-1}$ were obtained by varying silk concentration from 3.1% (w/w) to 12.4% (w/w). The variable silk concentration lyogels produced swelling ratios from 17.3 to 3.3. Silk densities of approximately 1000 g $(cm^3)^{-1}$ were obtained by pressing. The high density pressed matrices further reduced swelling ratios to 0.8 to 0.4.

The relationship between hydration and antibody recovery was characterized by comparing release to hydration from prior silk lyogel studies (Fig. 1D). The release/hydration data was well described empirically by the four parameter sigmoidal curve described in Equation (2).

$$y = y_0 + \frac{a}{1 + e^{-\left(\frac{x - x_0}{b}\right)}} \quad (2)$$

Fitting the data in Fig. 1D, the values of *a*, *b*, $y_0$and x_0 were determined to be 70.4, 1.7, 3.0 and 6.9, respectively. Maximum and minimum antibody recovery showed asymptotic behavior as a function of swelling ratio. Antibody recovery did not change significantly at swelling ratios below 3 and above 11. The most dynamic antibody recovery response was observed between swelling ratios of 3 and 11 with recoveries of approximately 10% and 67%, respectively. Based on the relationship described in Fig. 1D, the swelling ratio range above correlates to silk densities of approximately 60–185 g $(cm^3)^{-1}$.

3.2. Antibody release into variable release medium

To characterize the nature of interactions governing antibody release from lyogels, a series of experiments was performed evaluating the impact of various modifiers on antibody release. Three solution variables were investigated: surfactant levels, ionic strength and pH. The experiments relied on changing release medium rather than incorporating each modifier directly into the lyogel matrix to avoid altering the matrix itself. By only changing the release medium, a consistent starting point for each level of modifier was ensured. Silk lyogels at 6.8% (w/w) were used for these experiments because they demonstrated an intermediate release and recovery profile. Silk lyogels at 6.8% (w/w) were immersed into PBS at pH 7.4 with varying levels of the non-ionic surfactant polysorbate 80, 0.001%–1.0%. Increasing levels of polysorbate 80 incrementally increased the amount of antibody released from the lyogels (Fig. 2A). Antibody recovery improved from 39.5% in the absence of polysorbate 80 to 68.8% in the presence of 1.0% polysorbate in the release medium (Table 2). The swelling ratio increased from 6.4 to 8.3 with increasing polysorbate concentration (Table 2). Solution ionic strength was altered by increasing levels of sodium chloride in a 20 mM sodium phosphate solution at pH 7.4, including 150 mM, 300 mM, 1.5 M and 3.0 M. Increasing levels of sodium chloride incrementally decreased antibody release from the lyogels (Fig. 2B), from 40.8% in the absence of sodium chloride to 6.7% at 3 M sodium chloride. The swelling ratio decreased incrementally from 7.1 to 5.5 (Table 2). Solution pH was varied from 4.0 to 8.0 in 1.0 unit increments using a multi-component buffering system

(10 mM succinate, 10 mM histidine, 10 mM phosphate) to ensure comparable solution composition across the pH range. Decreasing the pH from 8.0 to 4.0 resulted in a significant and incremental reduction in antibody release (Fig. 2C), highest at pH 8.0 (39.9%) and lowest at pH 4.0 (4.6%) (Table 2). The swelling ratio remained constant across the pH range (Table 2).

Swelling ratio versus recovery results for each of the release media modifiers were overlaid with the sigmoidal model describing the hydration/recovery relationship (Fig. 2D-F). A linear regression was performed for the swelling/recovery data from each release media modifier. The analysis was intended primarily for visualization purposes, as insufficient data were available to determine linear fit with statistical validation. The empirical swelling/recovery slope with varying polysorbate 80 levels was similar to the model over the same swelling ratio range (Fig. 2D). In contrast, the empirical swelling/recovery slopes for sodium chloride (Fig. 2E) and pH (Fig. 2F) were significantly higher than the model over the same swelling ratio range.

3.3. Variable density silk lyogel and released antibody characterization

Temperature modulated differential scanning calorimetry (TMDSC) was performed to characterize bound water, glass transition and degradation of the varying density silk lyogels. Lyogels ranging in density from 48.6 g $(cm^3)^{-1}$ (3.1% (w/w)) to 950 g $(cm^3)^{-1}$ (6.7% (w/w) pressed) were evaluated from −50 °C to 350 °C. Two transitions were observed in the non-reversing heat flow thermograms (Fig. 3A). The first endothermic transition at approximately 75 °C is associated with the evaporation of bound non-freezing water [32]. The amount of residual water, measured by the transition enthalpy, did not change as a function of increasing silk density. While the enthalpy of the pressed sample water transition was similar to the control (unpressed samples), the peak width increased. The change in peak shape can be attributed to the increased packing density of the pressed matrix, making escape of the trapped water more difficult. The second, larger endothermic transition at approximately 275 °C represents the thermal degradation of the silk matrix. The degradation of the matrix occurred at similar temperatures regardless of silk density. A single endothermic transition at approximately 195 °C representing the glass transition of pure silk was observed in the reversing heat flow thermogram (Fig. 3B). No differences in the glass transition temperature were observed across the range of silk densities.

FTIR characterization was performed to understand if silk structure played a role in antibody release. The infrared (IR) region of 1700–1500 cm^{-1} corresponds to peptide backbone absorption for amide I (1700–1600 cm^{-1}) and amide II (1600–1500 cm^{-1}) bands. Absorbance spectra in this region are used for evaluating the secondary structure composition of various proteins, including silk fibroin [26,27]. Calculation of secondary structure composition through deconvolution of the amide I band was performed. Silk lyogels of varying density (Fig. 3C) and lyogels exposed to each modifier (Fig. 3D) were evaluated. In all samples silk lyogels demonstrated primarily β-sheet structure, accounting for approximately 60% of the structural composition. Neither increasing silk density (Fig. 3C) nor exposure to solution modifiers (Fig. 3D) significantly altered the structural composition.

3.4. Antibody stability and matrix modification

The chemical, physical, and functional stability of antibody released from variable density lyogels was evaluated. No significant instability was observed in post-encapsulated antibody samples (Fig. 4). The potency curves of loygel samples fell within the 95% confidence intervals describing the antibody control (Fig. 4A). Antibody samples released from silk lyogels contained mostly monomeric antibody, observed as a large peak on the SEC

chromatogram at 17.4 min (Fig. 4B). Antibody high molecular weight species content, peak at 15 min, remained unchanged at <1.5% in all samples. Increasing levels of low molecular weight species (LMWS) (19.5–24 min) were observed in released samples relative to the incubated antibody control. The increase in LMWS was confirmed to be a result of silk solubilizing over time (data not shown). Antibody secondary and tertiary structure was evaluated by far and near-UV CD spectroscopy respectively. A strong CD signal minimum was observed at approximately 217 nm in the far-UV consistent with the primarily β-sheet structure associated with antibodies. No differences were observed in the release antibody spectra compared to the incubated antibody control in either the far-UV (Fig. 4C) or near-UV (Fig. 4D) spectra. No changes in antibody fragmentation (Fig. 4E) or charge heterogeneity (Fig. 4F) were observed. For both gels, released antibody banding patterns were similar to that of the comparably incubated control.

Antibody oxidation was quantified by performing a tryptic digest followed by RP-HPLC to detect the oxidation marker peptide. Antibody oxidation was observed in a silk density dependent fashion (Fig. 5A). The incubated antibody control was 5.5% oxidized, increasing to 27.6% and 33.8%, for 3.1% and 6.7% silk lyogels, respectively. The addition of methionine as an anti-oxidant excipient significantly reduced the amount of antibody oxidation observed. Oxidation levels decreased to 9.3%, 7.3%, and 5.6% for 3 m_M, 10 m_M, and 30 m_M methionine levels, respectively (Fig. 5B).

4. Discussion

In the present study, we describe a systematic approach to elucidate the mechanistic basis for antibody release from a matrix material. The approaches utilized and the results reported provide methodology that is broadly applicable to other antibodies and other matrix systems. Further, the results lay out a strategy that can impact such systems and formulations in a more scientifically driven fashion, with broad implications for protein therapeutics including peptides, antibodies and related structures.

The direct impact of matrix density on antibody release and retention was small compared to the impact of water removal. Previous hydrogel work showed that increased silk density caused small decreases in antibody recovery and release rates [25]. Decreased hydrogel matrix porosity directly modified the diffusional component of antibody release from silk, while increased antibody–silk interactions led to decreased antibody recovery [18,25,33]. In contrast, antibody release and recovery decreased significantly upon lyophilization and subsequent hydration, making modification of hydration properties an attractive target for controlling release from silk lyogels.

Using swelling ratio as an indicator of hydration properties, a strong relationship between silk density and hydration was observed (Fig. 1C). Both approaches for altering silk matrix density, namely increased silk solution concentration or pressing, resulted in significant changes to the hydration properties. Differences in hydration behavior resulting from silk matrix density changes are independent of matrix structure as characterized by DSC and FTIR (Fig. 3). The primary mechanism of this relationship is likely the hydrophobicity of silk β-sheets that leads to the exclusion of water [34]. A high density network of hydrophobic, water excluding β-sheets, decreased the propensity for replacement water removed during lyophilization. Altering silk hydration and solubilization properties by various materials processing techniques such as water, solvent or vapor annealing has been previously demonstrated [28,35,36]. Similarly, silk matrix density is the primary parameter through which hydration properties of silk lyogels can be manipulated.

Lyogel hydration propensity is hypothesized to impact antibody release in two ways. The limited ability of the release medium to successfully penetrate the three dimensional matrix will directly impact antibody release. Also, a water-limited environment is not favorable for the reversal of silk-antibody interactions. Hydrophobic silk-antibody interactions replace silk-water and antibody–water interactions disrupted during the lyophilization process [25]. The sigmoidal relationship between lyogel swelling and antibody recovery (Fig. 1D) empirically describes the primary mechanism governing antibody release from silk lyogels – hydration resistance. A threshold hydration level is required for sufficient solvent penetration into the matrix to initiate antibody release. This threshold occurred at a swelling ratio of 3, corresponding to a silk density of approximately 185 mg $(cm^3)^{-1}$. Antibody recovery plateaued above a swelling ratio of 11, a silk density of approximately 60 mg $(cm^3)^{-1}$. The plateau indicates saturating levels of solvent penetration for maximum diffusional release and displacement of silk-antibody interactions.

To determine if hydration resistance is the sole parameter controlling antibody release and recovery a series of release media modification studies were performed. Polysorbate 80 (Fig. 2A) incrementally increased antibody recovery. In contrast, antibody recovery decreased while increasing levels of sodium chloride (Fig. 2B) or decreasing pH (Fig. 2C). The similarity in the empirical swelling/recovery slope for polysorbate 80 and variable matrix density samples (Fig. 2D) implies that antibody recovery was altered by modifying lyogel hydration properties in a manner consistent with silk matrix density changes. Empirical swelling/recovery slopes for sodium chloride and pH samples were significantly different from variable matrix density samples. This observation implies that swelling behavior had little effect on antibody release, indicating a secondary mechanism to hydration resistance.

Previous work, together with the results obtained in these studies, suggests a multi-modal mechanism controlling antibody release and recovery from silk lyogels (Fig. 6) [23,25,37]. Hydrophobic attraction is the primary driving force which traps the antibody preventing release. The ability to disrupt these interactions is governed by hydration resistance which in turn is controlled by silk matrix density. Repulsive ionic interactions, which mitigate the hydrophobic attraction, are a secondary mechanism. The isoelectric points for silk fibroin and the antibody are 4.5 and 5.0, respectively. At a physiological pH of 7.4 both molecules are negatively charged, resulting in a repulsive force. This counterbalance of hydrophobic attraction and ionic repulsion is diagrammed in the “normal” state (Fig. 6).

In the high silk density state water recovery is decreased. Therefore, the amount of water available for interaction with the matrix is decreased. Because of the limited solvent availability, silk antibody interactions are not readily displaced with silk-water and antibody–water interactions and an increase in antibody retention is observed. In the presence of polysorbate 80, hydrophobic regions are shielded. The primary effect is an increase in hydration as the amphiphilic polysorbate molecules bind to the most hydrophobic domains of the silk matrix facilitating the uptake of water. Polysorbate 80 is known to prevent protein–protein interactions and could therefore directly interfere with silk-antibody interactions facilitating release and recovery [38]. Neither variable silk density nor varying levels of polysorbate 80 had a detectable impact on silk matrix structure.

Antibody recovery behavior in the presence of sodium chloride and low pH both support the hypothesis of secondary ionic interactions. At high levels of sodium chloride, ionic repulsion is shielded, effectively increasing antibody retention through the hydrophobic attraction. At low pH, as both molecules approach their isoelectric point, their net negative charge neutralizes. In the absence of surface charge, the ionic repulsion is again eliminated, increasing the hydrophobic attraction [22]. No changes in silk matrix structure were observed after storage in high sodium chloride or low pH solutions.

Characterization of released antibody confirmed a favorable stability profile. No significant changes in physical stability, charge heterogeneity, or biological function were observed (Fig. 4). Interaction with the silk matrix was, however, found to induce antibody methionine oxidation (Fig. 5). The generation of reactive oxygen species by the energy and cavitation intensive sonication process combined with concentration effects during freezing and lyophilization may be responsible for the oxidative nature of the silk matrix [39,40]. While this chemical modification did not impact the biological activity of the model antibody, such a change is still concerning from the perspective of product quality, potential immunogenicity, and application to other protein therapeutics [8]. Lyogel matrix modification by the incorporation of methionine successfully mitigated this instability.

This mechanistic understanding identifies multiple control points for modifying antibody release and stability. Release could be controlled by altering either hydration or charge properties of the silk matrix. A variety of strategies, either individually or in combination, could be employed to manipulate these properties. The lyogel matrix could be modified indirectly by changing processing parameters such as silk pH, antibody pH, freezing rates, lyophilization cycle, and residual moisture or through the incorporation of excipients such as salts, surfactants, hydrophilic molecules or other modifiers to prevent silk-antibody interactions. Direct matrix modification could be accomplished through chemical modification or the introduction of a copolymer [41-45]. The therapeutic molecule could be selected or engineered with different hydrophobicity or surface charge to aid in optimization of the sustained local delivery system. Finally, the ability to effectively add stabilizing excipients directly to the matrix broadens the potential applicability of the system. With appropriate characterization, other classes of proteins, susceptible to different degradation pathways could be stabilized using this approach.

5. Conclusions

The mechanism controlling antibody release and recovery from silk lyogels has been determined. The strongest driving force was the hydration behavior of the silk lyogel matrix, which was controlled by silk matrix density. Limited solvent penetration and availability for the disruption of silk-antibody hydrophobic interactions decreased antibody recovery. Secondary ionic repulsions played a critical role in antibody recovery and release. Silk lyogels continue to be an attractive sustained delivery system for therapeutic proteins such as monoclonal antibodies. While difficult to fully characterize, delivery systems defined by multi-component release and stabilization mechanisms are desirable, offering a variety of possible control points. The gentle manufacturing process and lyophilized final dosage form create a device compatible with fragile protein therapeutics. The improved mechanistic understanding of silk-antibody interactions governing release, recovery, and stability presented here will aid in the engineering and formulation of silk lyogels to develop an optimized sustained delivery system for a given protein therapeutic.

Acknowledgments

The authors would like to acknowledge Carmen Preda and Jonathan Kluge for sharing their expertise in silk preparation and sonication, respectively. We are also grateful to Robert Simler and Robert Mattaliano for critically reviewing the manuscript and Alison Schroeer for editing the figures and producing the artwork used in Fig. 6. We also acknowledge funding of this work, which was provided by Genzyme and NIH grant EB002520.

References

[1]. Langer RS. Invited review: polymeric delivery systems for controlled drug release. Chem Eng Commun. 1980; 6:1–48.

[2]. Langer R. Drug delivery and targeting. Nature. 1998; 392:5–10. [PubMed: 9579855]

[3]. Brouwers JR. Advanced and controlled drug delivery systems in clinical disease management. Pharm World Sci. 1996; 18:153–62. [PubMed: 8933575]

[4]. Piggee C. Therapeutic antibodies coming through the pipeline. Anal Chem. 2008; 80:2305–10. [PubMed: 18456912]

[5]. Galluzzi L, Vacchelli E, Fridman WH, Galon J, Sautes-Fridman C, Tartour E, et al. Trial Watch: monoclonal antibodies in cancer therapy. Oncoimmunology. 2012; 1:28–37. [PubMed: 22720209]

[6]. Casi G, Neri D. Antibody-drug conjugates: basic concepts, examples and future perspectives. J Control Release. 2012; 161:422–8. [PubMed: 22306430]

[7]. Nelson AL, Dhimolea E, Reichert JM. Development trends for human monoclonal antibody therapeutics. Nat Rev Drug Discov. 2010; 9:767–74. [PubMed: 20811384]

[8]. Jiskoot W, Randolph TW, Volkin DB, Middaugh CR, Schoneich C, Winter G, et al. Protein instability and immunogenicity: roadblocks to clinical application of injectable protein delivery systems for sustained release. J Pharm Sci. 2012; 101:946–54. [PubMed: 22170395]

[9]. Uhrich KE, Cannizzaro SM, Langer RS, Shakesheff KM. Polymeric systems for controlled drug release. Chem Rev. 1999; 99:3181–98. [PubMed: 11749514]

[10]. Zhu G, Mallery SR, Schwendeman SP. Stabilization of proteins encapsulated in injectable poly (lactide-co-glycolide). Nat Biotechnol. 2000; 18:52–7. [PubMed: 10625391]

[11]. Sinha VR, Trehan A. Biodegradable microspheres for protein delivery. J Control Release. 2003; 90:261–80. [PubMed: 12880694]

[12]. Manning MC, Chou DK, Murphy BM, Payne RW, Katayama DS. Stability of protein pharmaceuticals: an update. Pharm Res. 2010; 27:544–75. [PubMed: 20143256]

[13]. Hawe A, Wiggenhorn M, van de Weert M, Garbe JH, Mahler HC, Jiskoot W. Forced degradation of therapeutic proteins. J Pharm Sci. 2012; 101:895–913. [PubMed: 22083792]

[14]. Rockwood DN, Preda RC, Yucel T, Wang X, Lovett ML, Kaplan DL. Materials fabrication from Bombyx mori silk fibroin. Nat Protoc. 2011; 6:1612–31. [PubMed: 21959241]

[15]. Panilaitis B, Altman GH, Chen J, Jin HJ, Karageorgiou V, Kaplan DL. Macrophage responses to silk. Biomaterials. 2003; 24:3079–85. [PubMed: 12895580]

[16]. Horan RL, Antle K, Collette AL, Wang Y, Huang J, Moreau JE, et al. In vitro degradation of silk fibroin. Biomaterials. 2005; 26:3385–93. [PubMed: 15621227]

[17]. Wang Y, Rudym DD, Walsh A, Abrahamsen L, Kim HJ, Kim HS, et al. In vivo degradation of three-dimensional silk fibroin scaffolds. Biomaterials. 2008; 29:3415–28. [PubMed: 18502501]

[18]. Hines DJ, Kaplan DL. Mechanisms of controlled release from silk fibroin films. Biomacromolecules. 2011; 12:804–12. [PubMed: 21250666]

[19]. Pritchard EM, Szybala C, Boison D, Kaplan DL. Silk fibroin encapsulated powder reservoirs for sustained release of adenosine. J Control Release. 2010; 144:159–67. [PubMed: 20138938]

[20]. Dyakonov T, Yang CH, Bush D, Gosangari S, Majuru S, Fatmi A. Design and characterization of a silk-fibroin-based drug delivery platform using naproxen as a model drug. J Drug Deliv. 2012; 2012:490514. [PubMed: 22506122]

[21]. Tsioris K, Raja WK, Pritchard EM, Panilaitis B, Kaplan DL, Omenetto FG. Fabrication of silk microneedles for controlled-release drug delivery. Adv Funct Mater. 2012; 22:330–5.

[22]. Hofer M, Winter G, Myschik J. Recombinant spider silk particles for controlled delivery of protein drugs. Biomaterials. 2012; 33:1554–62. [PubMed: 22079006]

[23]. Lu Q, Wang X, Hu X, Cebe P, Omenetto F, Kaplan DL. Stabilization and release of enzymes from silk films. Macromol Biosci. 2010; 10:359–68. [PubMed: 20217856]

[24]. Zhang J, Pritchard E, Hu X, Valentin T, Panilaitis B, Omenetto FG, et al. Stabilization of vaccines and antibiotics in silk and eliminating the cold chain. Proc Natl Acad Sci U S A. 2012; 109:11981–6. [PubMed: 22778443]

[25]. Guziewicz N, Best A, Perez-Ramirez B, Kaplan DL. Lyophilized silk fibroin hydrogels for the sustained local delivery of therapeutic monoclonal antibodies. Biomaterials. 2011; 32:2642–50. [PubMed: 21216004]

[26]. Dong A, Huang P, Caughey WS. Protein secondary structure in water from second-derivative amide I infrared spectra. Biochemistry. 1990; 29:3303–8. [PubMed: 2159334]

[27]. Dong A, Prestrelski SJ, Allison SD, Carpenter JF. Infrared spectroscopic studies of lyophilization- and temperature-induced protein aggregation. J Pharm Sci. 1995; 84:415–24. [PubMed: 7629730]

[28]. Lu Q, Hu X, Wang X, Kluge JA, Lu S, Cebe P, et al. Water-insoluble silk films with silk I structure. Acta Biomater. 2010; 6:1380–7. [PubMed: 19874919]

[29]. Mahler H-C, Friess W, Grauschopf U, Kiese S. Protein aggregation: pathways, induction factors and analysis. J Pharm Sci. 2009; 98:2909–34. [PubMed: 18823031]

[30]. Liu H, Gaza-Bulseco G, Sun J. Characterization of the stability of a fully human monoclonal IgG after prolonged incubation at elevated temperature. J Chromatogr B. 2006; 837:35–43.

[31]. Rapoza ML, Fu D, Sendak RA. Development of an in vitro potency assay for therapeutic TGF[beta] antagonists: the A549 cell bioassay. J Immunol Methods. 2006; 316:18–26. [PubMed: 17010369]

[32]. Hu X, Kaplan D, Cebe P. Effect of water on the thermal properties of silk fibroin. Thermochim Acta. 2007; 461:137–44.

[33]. Wang X, Hu X, Daley A, Rabotyagova O, Cebe P, Kaplan DL. Nanolayer biomaterial coatings of silk fibroin for controlled release. J Control Release. 2007; 121:190–9. [PubMed: 17628161]

[34]. Sohn S, Strey HH, Gido SP. Phase behavior and hydration of silk fibroin. Biomacromolecules. 2004; 5:751–7. [PubMed: 15132657]

[35]. Hu X, Shmelev K, Sun L, Gil ES, Park SH, Cebe P, et al. Regulation of silk material structure by temperature-controlled water vapor annealing. Biomacromolecules. 2011; 12:1686–96. [PubMed: 21425769]

[36]. Lawrence BD, Wharram S, Kluge JA, Leisk GG, Omenetto FG, Rosenblatt MI, et al. Effect of hydration on silk film material properties. Macromol Biosci. 2010; 10:393–403. [PubMed: 20112237]

[37]. Lu S, Wang X, Lu Q, Hu X, Uppal N, Omenetto FG, et al. Stabilization of enzymes in silk films. Biomacromolecules. 2009; 10:1032–42. [PubMed: 19323497]

[38]. Bee JS, Randolph TW, Carpenter JF, Bishop SM, Dimitrova MN. Effects of surfaces and leachables on the stability of biopharmaceuticals. J Pharm Sci. 2011; 100:4158–70.

[39]. Milowska K, Gabryelak T. Reactive oxygen species and DNA damage after ultrasound exposure. Biomol Eng. 2007; 24:263–7. [PubMed: 17353145]

[40]. Chang LL, Pikal MJ. Mechanisms of protein stabilization in the solid state. J Pharm Sci. 2009; 98:2886–908. [PubMed: 19569054]

[41]. Zhong T, Deng C, Gao Y, Chen M, Zuo B. Studies of in situ-forming hydrogels by blending PLA-PEG-PLA copolymer with silk fibroin solution. J Biomed Mater Res A. 2012; 100:1983–9. [PubMed: 22566401]

[42]. Hu X, Lu Q, Sun L, Cebe P, Wang X, Zhang X, et al. Biomaterials from ultrasonication-induced silk fibroin-hyaluronic acid hydrogels. Biomacromolecules. 2010

[43]. Vepari C, Matheson D, Drummy L, Naik R, Kaplan DL. Surface modification of silk fibroin with poly(ethylene glycol) for antiadhesion and antithrombotic applications. J Biomed Mater Res A. 2010; 93:595–606. [PubMed: 19591236]

[44]. Lu S, Wang X, Lu Q, Zhang X, Kluge JA, Uppal N, et al. Insoluble and flexible silk films containing glycerol. Biomacromolecules. 2010; 11:143–50. [PubMed: 19919091]

[45]. Wang S, Zhang Y, Wang H, Dong Z. Preparation, characterization and biocompatibility of electrospinning heparin-modified silk fibroin nanofibers. Int J Biol Macromol. 2011; 48:345–53. [PubMed: 21182858]

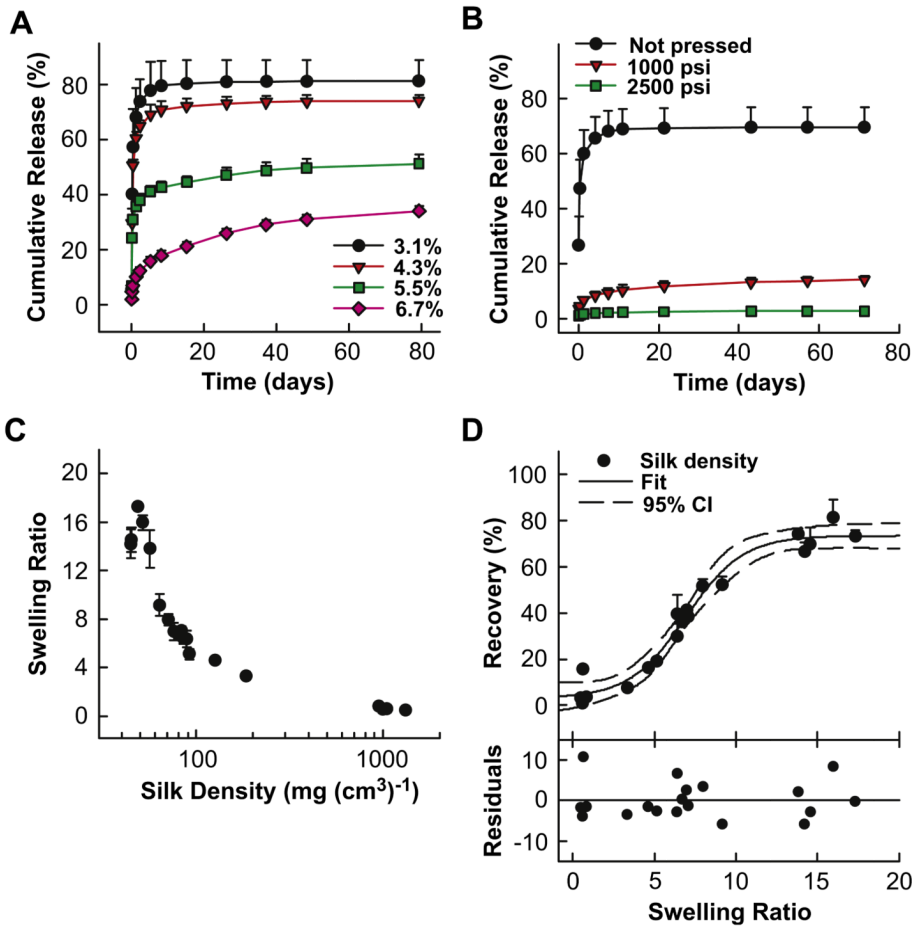

Fig. 1.

Variable silk matrix density studies. (A) Antibody release from variable matrix density produced by varying silk solution concentration from 3.1% (w/w) to 6.7% (w/w) representing silk densities from 52 mg $(cm^3)^{-1}$ to 80 mg $(cm^3)^{-1}$. (B) Antibody release from variable matrix density produced by pressing a 3.2% (w/w) silk lyogel representing silk densities from 45 mg $(cm^3)^{-1}$ to 1321 mg $(cm^3)^{-1}$. Release data was truncated at approximately 85% of cumulative release observed at plateau. Lines were added as a visual aid. (C) Silk lyogel hydration behavior modeled by swelling ratio as a function of silk matrix density. (D) Antibody recovery as a function of swelling ratio for variable density silk lyogels fit to a four parameter sigmoidal model. Residuals represent the difference between experimental and predicted values.

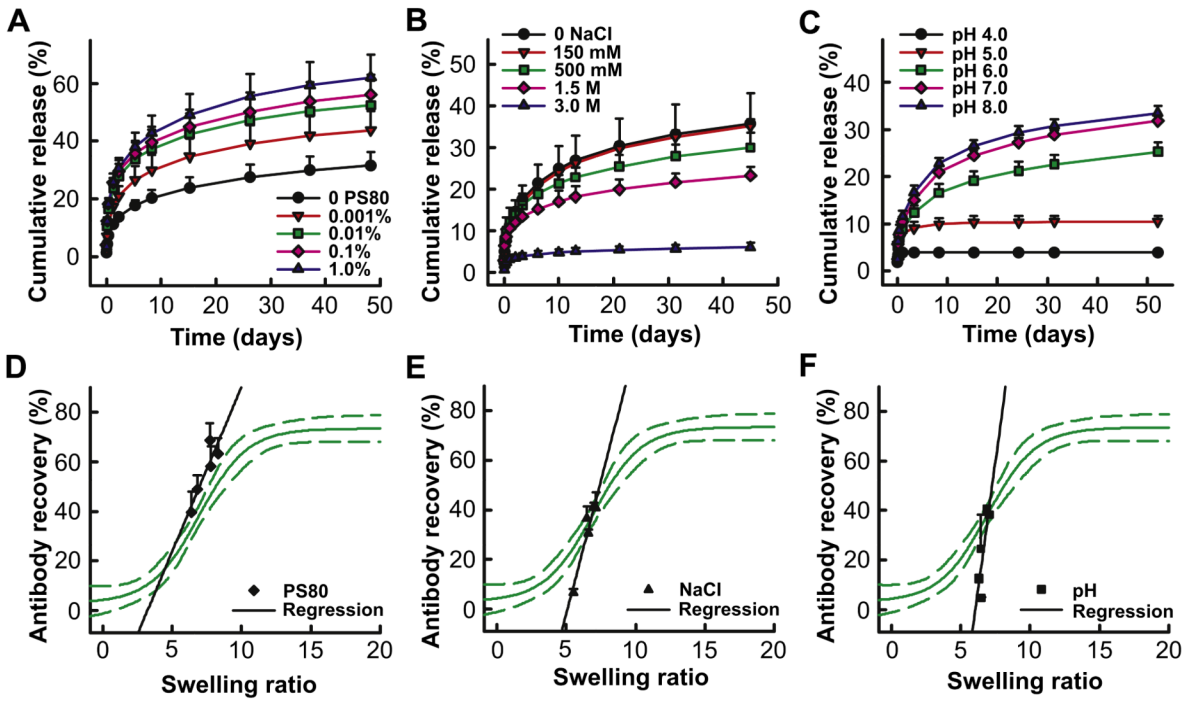

Fig. 2.

Variable release medium studies. Antibody release from silk lyogels as a function of variable release medium: (A) increasing levels of polysorbate 80, (B) increasing sodium chloride concentration, and (C) variable pH. Release data was truncated at approximately 85% of cumulative release observed at plateau. Lines were added as a visual aid. Antibody recovery as a function of swelling ratio for variable release medium: (D) variable polysorbate 80, (E) variable sodium chloride, and (F) variable pH compared to the model describing the recovery to swelling relationship for variable silk density.

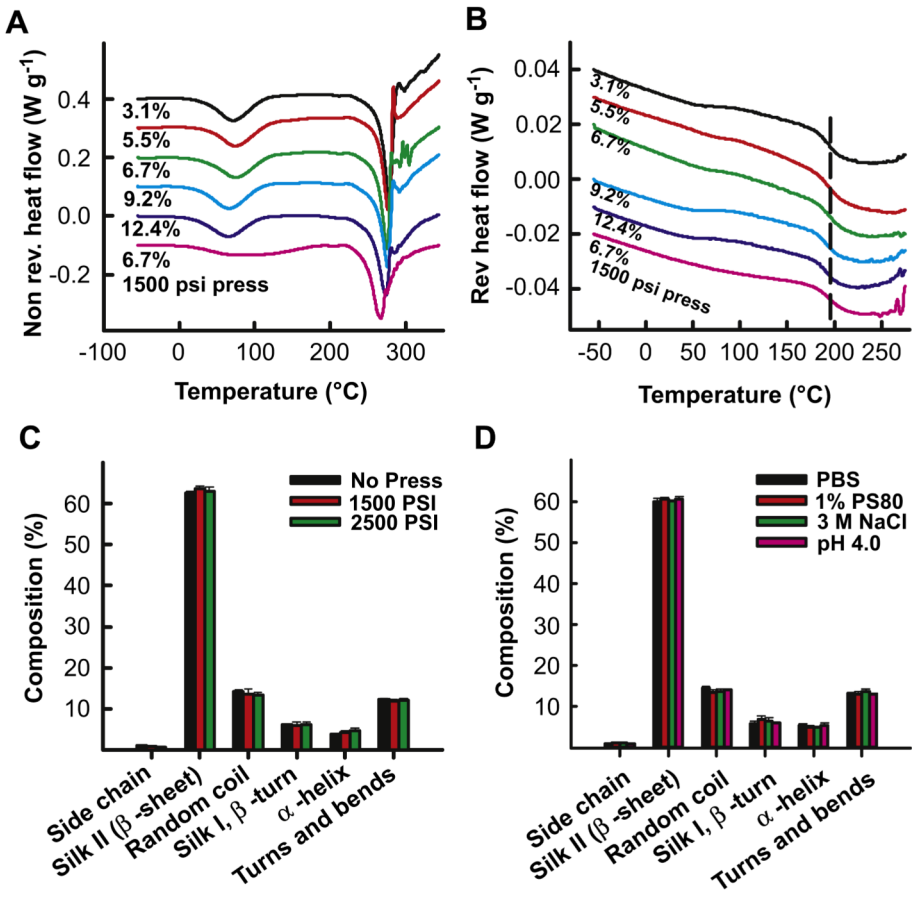

Fig. 3.

Structural characterization of silk lyogels. Thermal characterization of variable density silk lyogels by TMDSC with (A) non-reversing heat flow and (B) reversing heat flow thermograms. Secondary structure composition of silk lyogels determined by FTIR for (C) variable silk density and (D) after exposure to various release medium conditions.

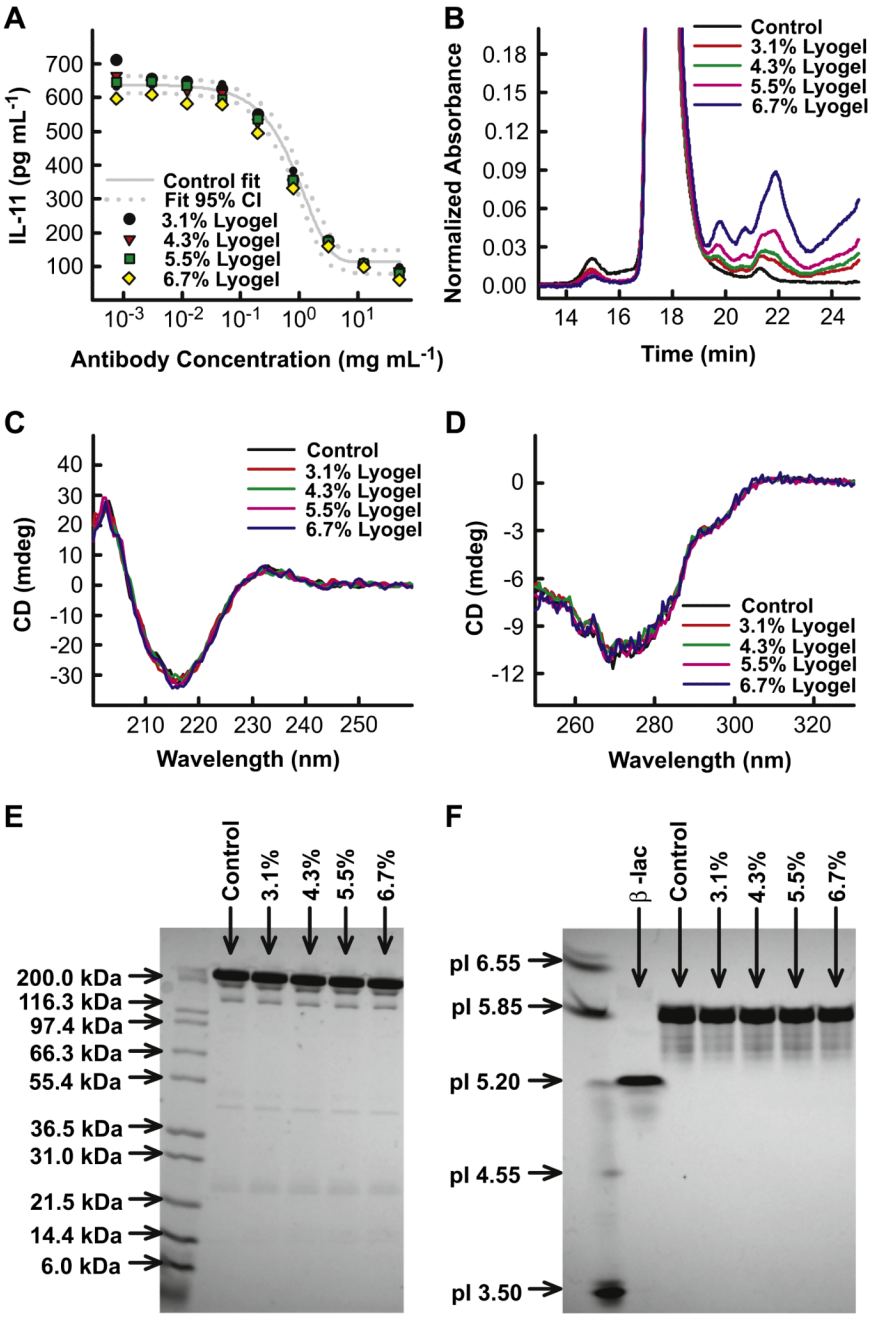

Fig. 4.

Stability characterization of antibody released from variable concentration lyogels. (A) Antibody potency represented by IL-11 inhibition dose response curves. (B) SEC chromatogram overlays evaluating antibody aggregation and fragmentation. (C) Antibody (C) secondary and (D) tertiary structure evaluated by far-UV CD and near-UV CD, respectively. (E) Fragmentation determined by non-reduced SDS-PAGE.

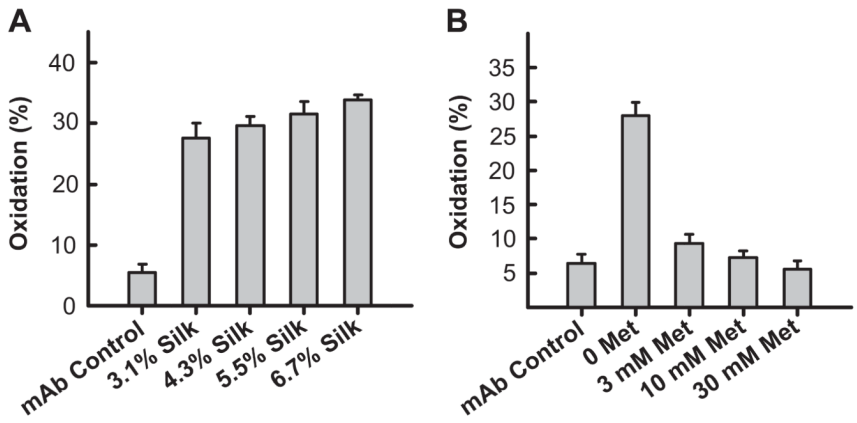

Fig. 5.

Lyogel modification with methionine to control antibody oxidation. (A) Calculated oxidized methionine marker peptide levels in antibody samples released from variable concentration lyogels. (B) Calculated oxidized methionine marker peptide levels in antibody samples released from 3.1% (w/w) lyogels with varying methionine levels incorporated into the matrix.

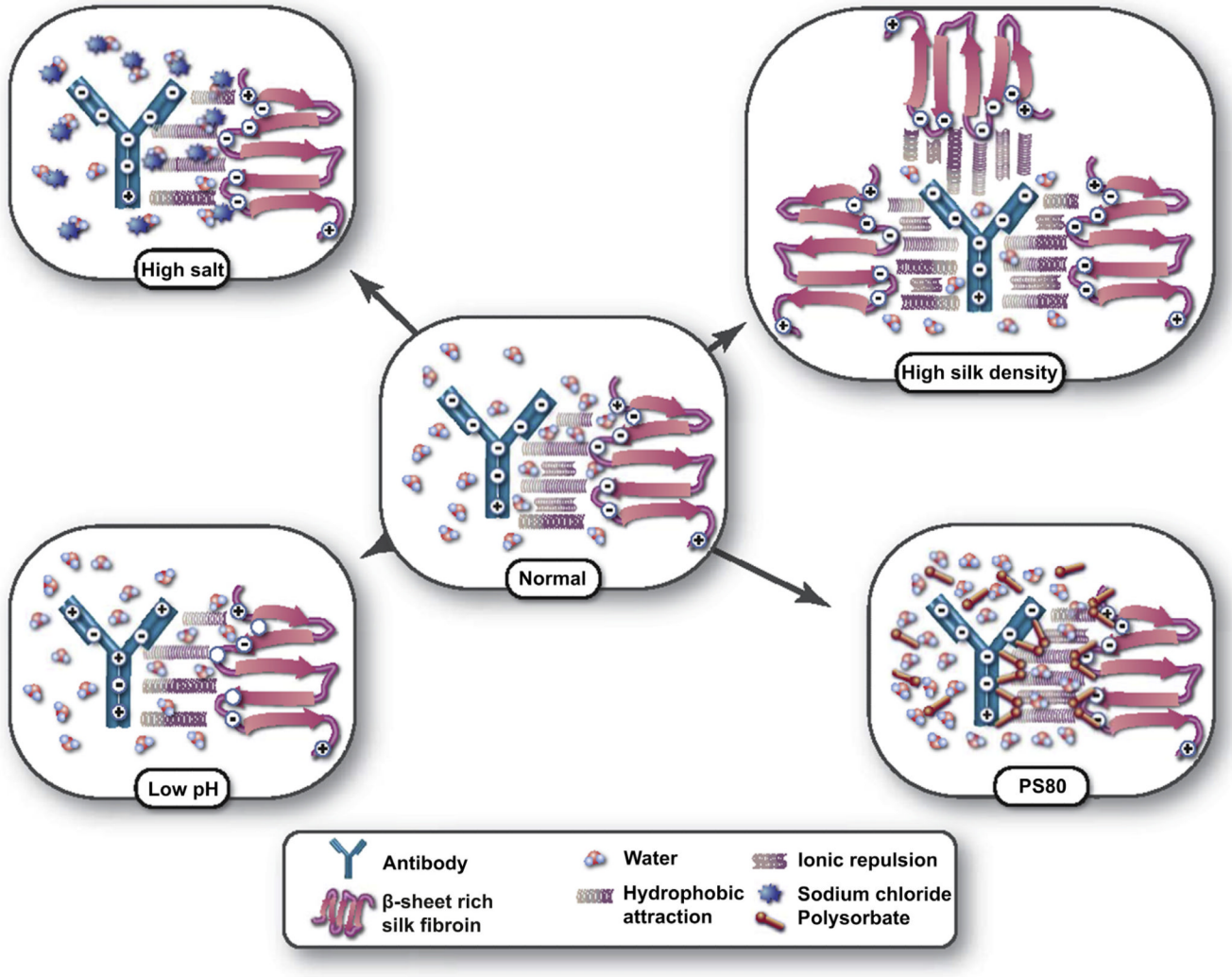

Fig. 6.

Schematic representation of silk-antibody interactions governing release and recovery. In the normal condition (physiological PBS) hydrophobic attraction combined with an opposing ionic repulsion control antibody release. In the high silk density state hydration is decreased minimizing the disruption of hydrophobic interactions decreasing recovery. Addition of polysorbate 80 increases hydration and shields hydrophobic interactions improving recovery. High salt and low pH decrease recovery by eliminating the repulsive forces through ionic shielding and charge neutralization, respectively.

Table 1

Numerical summary of swelling and antibody recovery from variable silk density lyogels

Sample	Silk density (mg $(cm^3)^{-1}$)	Swelling ratio	Antibody recovery (%)
3.1% silk	51.6 (±2.6)	16.0 (±0.6)	81.3 (±7.7)
4.3% silk	56.4 (±2.7)	13.8 (±1.6)	74.2 (±2.3)
5.5% silk	63.3 (±1.8)	9.1 (±0.9)	52.2 (±3.5)
6.7% silk	80.4 (±5.1)	6.7 (±0.3)	36.0 (±2.0)
Not pressed	44.9 (±3.7)	14.5 (±1.0)	69.8 (±7.2)
1500 psi	1045.3 (±36.8)	0.6 (±0.01)	15.6 (±1.6)
2500 psi	1320.5 (±40.5)	0.5 (±0.08)	3.0 (±0.6)

Table 2

Numerical summary of swelling and antibody recovery from variable release medium silk lyogels.

Sample	Silk density (mg $(cm^3)^{-1}$)	Swelling ratio	Antibody recovery (%)
0PS80	85.3 (±4.8)	6.4 (±0.4)	39.5 (±8.4)
0.001% PS80	81.0 (±1.6)	6.8 (±0.4)	48.8 (±5.9)
0.01% PS80	88.0 (±4.2)	7.8 (±0.5)	58.1 (±8.3)
0.1% PS80	83.2 (±2.6)	8.3 (±0.7)	63.4 (±6.3)
1.0% PS80	85.1 (±3.2)	7.7 (±0.4)	68.8 (±6.7)
0 mM NaCl	79.4 (±4.1)	7.1 (±0.1)	40.8 (±6.3)
150 mM NaCl	75.8 (±2.7)	7.0 (±0.7)	41.2 (±1.8)
500 mM NaCl	76.7 (±3.7)	6.5 (±0.2)	36.6 (±4.9)
1.0 M NaCl	74.5 (±1.4)	6.6 (±0.4)	30.5 (±1.6)
3.0 M NaCl	77.1 (±3.2)	5.5 (±0.4)	6.7 (±1.3)
pH 4.0	76.2 (±1.8)	6.5 (±0.5)	4.6 (±0.5)
pH 5.0	81.6 (±6.1)	6.3 (±0.5)	12.3 (±1.5)
pH 6.0	85.6 (±6.9)	6.5 (±0.4)	30.6 (±2.4)
pH 7.0	83.3 (±0.6)	7.1 (±0.4)	38.2 (±1.3)
pH 8.0	85.6 (±5.8)	6.9 (±0.2)	39.9 (±1.8)